Group B Streptococcal β-Hemolysin Induces Nitric Oxide Production in Murine Macrophages

Axel Ring,[1,a] Johann S. Braun,[1,a] Victor Nizet,[4] Wolfgang Stremmel,[3] and Jerry L. Shenep[1,2]

[1]Department of Infectious Diseases, St. Jude Children's Research Hospital, and [2]Department of Pediatrics, University of Tennessee, Memphis; [3]Department of Internal Medicine IV, Ruprecht-Karls-University, Heidelberg, Germany; [4]Division of Pediatric Infectious Diseases, University of California, San Diego

Group B streptococcus (GBS) is the leading cause of sepsis in neonates. Nitric oxide (NO) release plays a role in the hypotension that characterizes septic shock. To examine the role of the GBS β-hemolysin in NO production, the murine macrophage line RAW 264.7 was exposed to a wild-type (WT) GBS isolate and to hyperhemolytic (HH) and nonhemolytic (NH) transposon mutants derived from that isolate. After activation of macrophages by the WT strain, the HH mutant, or cell-free extracts of β-hemolysin, nitrite release into the supernatant increased >10-fold and inducible NO synthase (iNOS) levels in cell lysates increased up to 10-fold compared with treatment with the NH mutant or extracts from that mutant. Hemolysin-induced NO production was dependent on protein tyrosine kinases and NF-κB, but not on extracellular signal-related kinase-1/2–mitogen-activated kinases or protein kinase A. These results indicate that GBS β-hemolysin induces murine macrophage iNOS via intracellular pathways similar to those that mediate lipopolysaccharide-induced iNOS activation.

Group B streptococcus (GBS; *Streptococcus agalactiae*) is the leading cause of pneumonia, meningitis, and septic shock in newborns, particularly those born prematurely [1]. All clinical isolates are encapsulated, and 98%–99% are β-hemolytic [2]. The GBS capsular polysaccharide contributes to virulence by virtue of its antiphagocytic property [3]. The GBS β-hemolysin, a potent membrane cytotoxin that injures lung epithelial [4] and endothelial [5] and brain endothelial [6] cells, may contribute to the pathogenesis of neonatal pneumonia and meningitis. Crude β-hemolysin preparations from GBS cultures induce cardiotoxicity and hypotension after intravenous administration to rabbits or rats, suggesting a role in septic shock [7]; however, the molecular mechanisms by which the GBS β-hemolysin may contribute to the pathogenesis of septic shock have not been delineated.

The hypotension of septic shock is thought to be due in part to an excess production of nitric oxide (NO), as elevated NO levels are found in septic patients [8, 9]. Three isoforms of NO synthases (NOS) are present in mammals: the high-output inducible NOS (iNOS) and two constitutive isoforms, one originally identified in neurons (ncNOS) and the other in endothelial cells (ecNOS). iNOS is not expressed by resting cells but is readily induced in permissive cells upon stimulation by proinflammatory cytokines, lipopolysaccharide (LPS), or other bacterial cell wall components [10, 11]. Large constant amounts of NO are released by activated macrophages after iNOS induction, accounting in part for the antimicrobial properties of these cells [12]. Fibroblasts, Kupffer cells, hepatocytes, renal epithelium, chondrocytes, glial cells, smooth muscle cells, cardiac myocytes, and endothelial cells also can express iNOS under diverse pathophysiologic conditions [13–20]. In animal models of septic shock, circulatory failure has been associated with enhanced NO production, most conspicuously via iNOS [21]. In contrast, the relatively small amounts of NO produced by the low-output constitutive NOSs appear to be organ protective during the early, hyperdynamic phase of septic shock [21]. Nonetheless, ecNOS activity can be precipitously enhanced by cytokines, LPS, *Staphylococcus aureus* lipoteichoic acid (LTA), and the pore-forming hemolysins of *S. aureus* and *Escherichia coli* [10, 22, 23].

GBS induces NO production in murine macrophages by a CD11b/CD18 receptor-mediated process [24]. However, the specific GBS factor(s) responsible for inducing iNOS in sepsis has not been identified. Cell wall preparations derived from other streptococci induce NO production, but at doses rarely encountered in clinical practice [25]. We recently found that pneumolysin, a hemolysin produced by *Streptococcus pneumoniae,* induces iNOS in murine macrophages [25]. On the basis of this novel observation, we hypothesized that the GBS β-hemolysin may also activate iNOS, although this hemolysin is

Received 22 October 1999; revised 10 March 2000; electronically published 30 June 2000.

Financial support: National Institutes of Health (AI-27913 to J.L.S.; AI-01451 to V.N.); Cancer Center Support grant CA-21765; American Lebanese Syrian Associated Charities.

[a] Present affiliations: Department of Internal Medicine IV, Ruprecht-Karls-University, Heidelberg, Germany (A.R.); Department of Neurology, Humboldt University, Berlin, Germany (J.S.B.).

Reprints or correspondence: Dr. Jerry L. Shenep, Dept. of Infectious Diseases, St. Jude Children's Research Hospital, 332 N. Lauderdale St., Memphis, TN 38105-2794 (jerry.shenep@stjude.org).

The Journal of Infectious Diseases 2000; 182:150–7

0022-1899/2000/18201-0019$02.00

not a member of the cholesterol-binding, sulfhydryl-activated, pore-forming hemolysin family that includes pneumolysin and streptolysin O [26]. In the present study we investigated the role of the GBS β-hemolysin in the induction of iNOS and NO production in RAW 264.7 macrophages and the macrophage intracellular signaling pathways by which GBS-mediated iNOS induction occurs.

Materials and Methods

Materials. Dulbecco's MEM (DMEM), L-glutamine, and fetal bovine serum (FBS), containing <0.1 endotoxin units (EU)/mL, and the chromogenic limulus amebocyte lysate (LAL) assay were purchased from BioWhittaker (Walkersville, MD). LPS purified from *E. coli* O111:B4, polymyxin B sulfate, recombinant mouse interferon (IFN)–γ aprotinin, sodium vanadate, leupeptin, Triton-X 100, phenylmethylsulfonyl fluoride (PMSF), MTT, the assay kit for lactate dehydrogenase (LDH), the components of the Griess reagent, and the C+Y medium constituents [27] were purchased from Sigma Chemical (St. Louis). All signal transduction inhibitors were purchased from Calbiochem (La Jolla, CA). Human serum albumin intended for use in patients was obtained from Immuno US (San Diego).

Bacterial strains. COH1, an encapsulated type III strain of GBS isolated from the blood of a septic neonate [28], was used in this study. Mutants COH1-20 (nonhemolytic, NH) and IN40 (hyperhemolytic, HH) are isogenic derivatives of strain COH1, and each contains a single insertion of Tn916ΔE into its chromosome [4]. Bacteria were maintained and grown to late logarithmic phase (OD of 1.0, corresponding to 2.5×10^8 cfu/mL) in the semisynthetic medium C+Y, which did not contain any detectable contaminating endotoxin (<0.05 EU/mL) as assessed by the chromogenic LAL test.

Preparation of stabilized hemolysin extracts. From logarithmic growth in C+Y, 8 L of culture medium containing ~ 2.5×10^8 cfu/mL was pelleted at 3000 *g* for 10 min at 4°C, washed twice in PBS, and resuspended in 200 mL of cell culture medium supplemented with 5% human serum albumin and 0.2% starch as required to stabilize hemolytic activity [29]. After the suspension was incubated for 10 min at 37°C and centrifuged at 3000 *g* for 10 min at 4°C, the supernatant (hemolysin extract) was passed through a 0.22-μm filter for sterilization. The extracts were kept on ice after the procedure for ≤1 h prior to use or frozen at −20°C and used in subsequent experiments.

Assay for hemolytic activity. A modification of the method of Marchlewicz and Duncan [29] was used to quantify GBS hemolysin activity using whole bacteria and the albumin/starch-stabilized hemolysin extracts. From logarithmic growth in C+Y, 10^8 cfu of GBS was pelleted by centrifugation at 3000 *g,* washed once with PBS, and resuspended in PBS at a concentration of 1.2×10^8 cfu/mL. The time dependence of hemolysis induced by live GBS was demonstrated by incubation of 3% sheep erythrocytes with a suspension of 1.2×10^8 cfu/mL of GBS for the time points indicated in a 5% CO_2 atmosphere in a total volume of 200 μL at 37°C. PBS alone and double-distilled water (hypotonic lysis) were used as negative and positive controls, respectively. After incubation, 150 μL of the GBS-erythrocyte mixture was transferred to a 1.5-mL tube containing 650 μL of PBS and spun for 7 min at 1500 rpm in a microcentrifuge. The supernatant was analyzed for the presence of released hemoglobin by measurement of the absorption at 415 nm. To determine the hemolytic titer of stabilized GBS hemolysin extracts, the extracts were serially diluted 2-fold and incubated with 3% sheep erythrocytes for 1 h at 37°C in 5% CO_2, and the release of hemoglobin was determined as described above. The hemolytic activity of a bacterial strain or hemolysin extract was expressed in hemolytic units (HU), defined as the reciprocal of the greatest dilution producing 50% hemoglobin release compared with the positive control. All assays were performed in duplicate and repeated three times.

Murine macrophage cell cultures. RAW 264.7 cells (American Type Culture Collection, Rockville, MD) were maintained and passaged in DMEM supplemented with 4 m*M* glutamine and 10% FBS. All materials were purchased from BioWhittaker and assayed for the presence of contaminating endotoxin by the LAL test prior to use in the experiments. Nitrite release was determined in 96-well plates with 10^5 cells per single well in 200 μL of medium seeded 1 h before the experiment.

Nitrite assay. Quantification of nitrite, the stable product of NO, was done with the Griess reaction as described elsewhere [30]. After activation of RAW 264.7 cells for 18 h, the 96-well plates were centrifuged at 3000 *g* for 10 min to pellet bacteria, and 100 μL of the supernatant was transferred to a replica plate. We added 50 μL of 0.1% *N*-1-naphthyl-ethylenediamine–HCl and 50 μL of 1% sulfanilamide in 5% H_3PO_4 to each well, and plates were read in a spectrophotometric plate reader at 543 nm after 5 min. Nitrite concentrations were determined with a standard curve.

MTT assay. After 18 h of exposure to GBS or hemolysin extracts, the MTT assay for cell viability was done as described elsewhere [31]. This assay is based on the reduction of colorless MTT to tetrazolium blue crystals by viable cells. Acid isopropanol (0.04 *N* HCl) was added to the wells to solubilize the tetrazolium blue crystals. Absorption at 540 nm was measured with a spectrophotometric plate reader. Cytotoxicity was calculated as follows: % cytotoxicity = 100 × (absorb sample − absorb without cells) / (absorb control − absorb without cells), where "absorb" is absorbance of the sample well, "absorb without cells" is absorbance with no cells present, and "absorb control" is the absorbance of wells with no treatment.

LDH assay. Cell injury was also assessed by the release of LDH into the culture medium during the 18-h incubation of RAW 264.7 cells with GBS or LPS. The LDH activity in cell culture media and cell lysates was determined by a colorimetric assay (Procedure 500; Sigma) for pyruvate with the amount of residual pyruvate being inversely proportional to the amount of LDH activity. The LDH release is expressed as the ratio of LDH activity in experimental wells compared with wells with no treatment.

Western blot analysis. RAW 264.7 cells that were exposed to GBS or medium were washed, scraped, pelleted by centrifugation, and lysed with ice-cold 50 m*M* Tris-HCl (pH 7.6) containing 1% Triton-X 100, 1 m*M* EDTA, 1 m*M* sodium vanadate, 0.1 mg/mL PMSF, and 10 μg/mL leupeptin. The lysate was centrifuged for 10 min at 4°C in a microcentrifuge. The proteins in the supernatant were separated by SDS-PAGE and transferred to nitrocellulose paper for Western blotting. After blocking in pH 7.4 Tris-buffered saline (TBS) with 5% bovine serum albumin and 0.2% Tween at

room temperature for 3 h, blots were washed with TBS and incubated with a 1:2000 dilution of the primary mouse anti-iNOS antibody for 1 h. After being washed, the blots were incubated with a secondary antibody, a peroxidase-conjugated goat anti–mouse IgG. After another wash, the blots were developed using the ECL kit (Amersham, Amersham, UK), a chemiluminescent substrate for horseradish peroxidase. The resulting luminescence was detected by exposure to x-ray film and quantified by densitometer.

Results

Time course of hemolysis by GBS strains. We investigated the time course of hemolysis caused by GBS clinical isolate COH1 (WT) and isogenic mutants exhibiting an NH (COH1-20) or HH (IN40) phenotype. The growth rates of the WT and HH strains in the erythrocyte suspension were comparable, whereas growth of NH was ~20% delayed (data not shown). The HH mutant caused complete lysis of a 3% sheep erythrocyte suspension within 20 min. In contrast, the WT strain required 2 h to initiate and 6 h to complete red blood cell lysis. The NH strain did not produce detectable lysis of erythrocytes after >1 day.

Dose dependence of nitrite accumulation by RAW 264.7 cells upon stimulation by GBS. Replicating hemolytic GBS caused death of RAW 264.7 cells when incubated for 18 h at 37°C independent of the initial dose. Therefore, we added an inhibitory but not bactericidal concentration of chloramphenicol (50 μg/mL) to the incubation medium to abrogate bacterial growth. IFN-γ alone at a dose of 5 U/mL did not result in nitrite accumulation in RAW 264.7 cell supernatants after 18 h of incubation. As shown in figure 1, the HH mutant induced ~10 μmol/L nitrite after 18 h of incubation with IFN-γ–primed RAW 264.7 cells. Peak induction was seen at bacterial concentrations of 1 to 2.5×10^6 cfu/mL. Higher bacterial concentrations resulted in less nitrite accumulation. This decrease may be due to macrophage cytotoxicity, which was demonstrated by increased LDH release and decreased activity in the MTT cell viability assay at the higher bacterial concentrations (data not shown).

Exposure of naive (not IFN-γ–primed) RAW 264.7 cells to the HH mutant resulted in about 2-fold less (5 μmol/L) nitrite accumulation than with the combined GBS/IFN-γ treatment. As with the IFN-γ–treated cells, the peak induction occurred at bacterial concentrations between 1 and 2.5×10^6 cfu/mL. Cytotoxicity was also evident in naive cells at higher GBS concentrations; however, the decline of nitrite accumulation was less pronounced than in the IFN-γ–primed cells, suggesting that the cytotoxicity of HH GBS is enhanced in the presence of IFN-γ. Consistent with this hypothesis, increased LDH release was observed from RAW 264.7 cells exposed to HH GBS/IFN-γ compared with those exposed to HH GBS alone (data not shown).

Exposure to the relatively less hemolytic WT strain resulted in similar peak levels of NO accumulation; however, higher doses of bacteria were required to induce peak NO production ($\sim 6 \times 10^6$ cfu/mL vs. 10^6 cfu/mL). At high bacterial concentrations, the absolute levels of nitrite released from macrophages exposed to the WT GBS were greater than seen with the HH mutant (figure 1), possibly because the enhanced cytotoxicity of the HH mutant diminished the ability of the RAW cells to produce NO. The NH mutant was unable to induce nitrite accumulation at doses up to 12×10^6 cfu/mL independent of priming by IFN-γ (figure 1). Higher concentrations of the NH mutant induced nitrite at a low level (data not shown), perhaps because of an effect of bacterial cell wall components on the activation of iNOS.

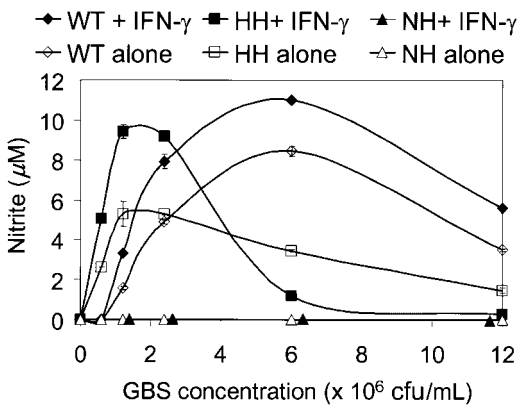

Figure 1. Dose dependence of group B streptococcus (GBS)–activated nitric oxide (NO) production by RAW 264.7 macrophages. 10^5 Cells per well in 96-well plate were incubated with varying doses of GBS strains wild-type (WT), hyperhemolytic (HH), and nonhemolytic (NH) for 18 h at 37°C. NO release was measured as accumulated nitrite. *Open symbols,* cells not treated with interferon (IFN)–γ; *closed symbols,* results from cells treated with 5 U/mL murine IFN-γ beginning 4 h before GBS challenge. Data are mean ± SD (*bars,* in some cases obscured by data markers due to small SDs of data sets) of accumulated nitrite in culture medium in 3 independent experiments. Data for individual experiments are means of duplicate measurements.

Contaminating LPS was not detected in the bacterial culture medium (C+Y) or the assay medium by the quantitative LAL test. Also, the accumulation of nitrite in response to GBS was unaffected by addition of polymyxin B (10 μg/mL), which binds and inactivates LPS, in the assay medium (data not shown).

Time dependence of iNOS expression by RAW 264.7 cells upon stimulation by GBS and IFN-γ. To confirm that NO was produced by iNOS in our system and to study the time course of iNOS activation, we challenged IFN-γ–primed RAW 264.7 cells with GBS for periods of 3–18 h and performed Western blots on cell lysates, using a monoclonal iNOS antibody. As shown in figure 2, the expression of iNOS protein was earliest and strongest in macrophages activated with the HH mutant at a concentration of 2.5×10^6 cfu/mL. The expression of iNOS protein was first detectable by 6 h and peaked at 18 h. In contrast, exposure to the NH mutant at the same bacterial

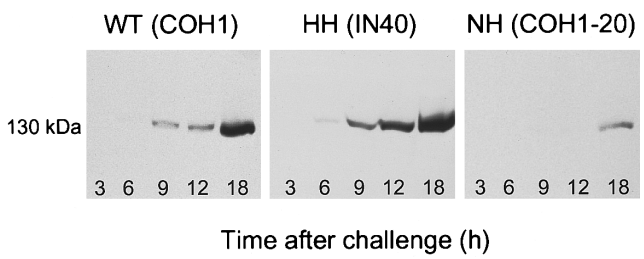

Figure 2. Time course of inducible nitric oxide synthase (iNOS) protein expression in group B streptococcus (GBS)–activated RAW 264.7 macrophages. 4×10^6 Cells in 25-cm^2 flask were incubated with 4×10^7 cfu of GBS (strains wild-type [WT], hyperhemolytic [HH], or nonhemolytic [NH]) and chloramphenicol (50 μg/mL) at 37°C. Cells were treated with 5 U/mL interferon-γ beginning 4 h before GBS challenge. At times indicated (hr), cell monolayers were washed and Western blots done on cell lysates separated by SDS-PAGE.

concentration resulted in a delayed and low-level iNOS response that was not initiated until 12 h after challenge. Compared with HH and NH, the WT strain displayed an intermediate ability to induce iNOS; the protein expression commenced after 9 h and peaked after 18 h.

Dose dependence of nitrite production by RAW 264.7 cells upon stimulation by cell-free hemolysin-containing extracts. To assess the contribution to RAW 264.7 cell nitrite production of β-hemolysin relative to other secreted bacterial components, bacteria-free albumin/starch-stabilized supernatants from log phase GBS were prepared from cultures of the HH and NH mutants. The average hemolytic activity of supernatant preparations from HH cultures was 50 HU, whereas the control supernatant preparations from the NH mutant had no detectable hemolytic activity (no activity undiluted, <1 HU). The nitrite accumulation produced by the stabilized hemolysin extracts from the HH mutant peaked at a dilution of 1:5, corresponding to an activity of 10 HU. In contrast, the control preparation from the NH mutant produced little if any nitrite accumulation at a 1:5 dilution (data not shown). The 1:2 dilution of the HH extract (corresponding to 25 HU) induced less nitrite than the 1:5 dilution, consistent with the cytotoxic effects of the HH supernatant in the MTT and LDH assays. NO release induced by the NH mutant extract at the lowest (1:2) dilution is presumably due to nonhemolytic bacterial components (e.g., cell wall products) released into the supernatant. Nonstabilized hemolysin extracts from the WT and HH strains had markedly diminished NO-inducing activity (data not shown), comparable to the NH mutant extracts, indicating that β-hemolysin was the source of activity.

The effect of signal transduction inhibitors on nitrite formation by GBS-treated RAW 264.7 macrophages. Signal transduction inhibitors were used to compare the mechanism of NO production by GBS β-hemolysin to that by LPS, the prototypic inducer of NO production in RAW 264.7 and other macrophages. The intracellular pathways investigated are outlined in figure 3. The tyrosine kinase inhibitors genistein (figure 4*A*), herbimycin A (not shown), and tyrphostin AG126 (not shown) reduced nitrite formation induced by WT GBS and LPS, either alone or in the presence of IFN-γ, in a concentration-dependent manner, suggesting a role for one or more of the tyrosine kinases shown in figure 3. The maximal inhibition was produced by tyrphostin AG126 at 50 μM (73.1% ± 11.4% without and 88.9% ± 11.2% with IFN-γ) and by genistein at 100 μM (figure 4*A*), whereas the maximal inhibition of nitrite formation mediated by herbimycin A was at 1 μM (66.9% ± 24.2% without and 71.4% ± 10.0% with IFN-γ). Genistein appeared to more effectively inhibit GBS-induced than LPS-induced nitrite release (figure 4*A*), whereas tyrphostin AG126 and herbimycin A were equipotent inhibitors of both LPS- and GBS-induced NO production (not shown). Tyrphostin A-1, an inactive analogue of tyrphostin AG126, or daidzein, an inactive analogue of genistein (both tested up to a concentration of 50 μM), did not significantly alter the formation of nitrite after GBS or LPS stimulation (data not shown). The solvent used to dissolve the tyrosine kinase inhibitors, dimethyl sulfoxide, did not affect the nitrite formation induced by GBS or LPS at the maximum concentration used, 0.05%. The effect of inhibitors on cell viability in our assays was monitored by the MTT test and by measurement of LDH in the supernatant. In all assays shown in figure 4, the reduction of MTT was always ⩾90%, and the accumulation of LDH was never >10% compared with control wells without inhibitor.

The increase in nitrite formation caused by GBS or LPS was inhibited in a concentration-dependent manner by pyrrolidine

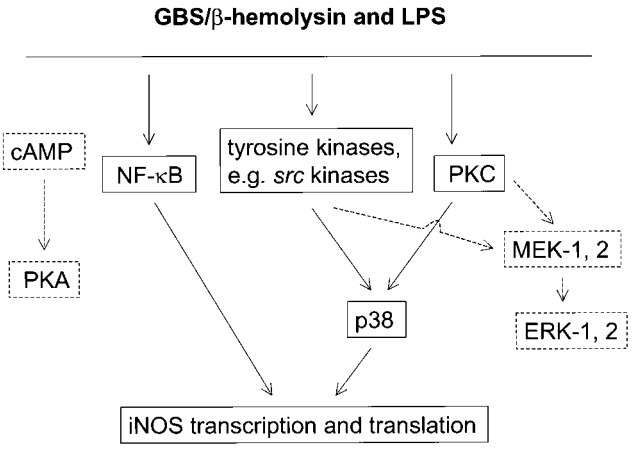

Figure 3. Signaling pathways investigated for potential role in inducible nitric oxide (NO) synthase (iNOS) induction. Inhibition of pathways *(solid lines)* reduced NO production upon stimulation with either lipopolysaccharide (LPS) or group B streptococcus (GBS)/β–hemolysin extract (see figure 4). Inhibition of other pathways *(dashed lines)* did not affect NO production induced by LPS or GBS/β-hemolysin extract. PKC and PKA (protein kinases C and A, respectively); mitogen activated protein kinase (MAPK)/extraceullar signal-related kinase (ERK) 1, 2 (MEK-1, 2); ERK-1 and -2 (ERK-1, 2).

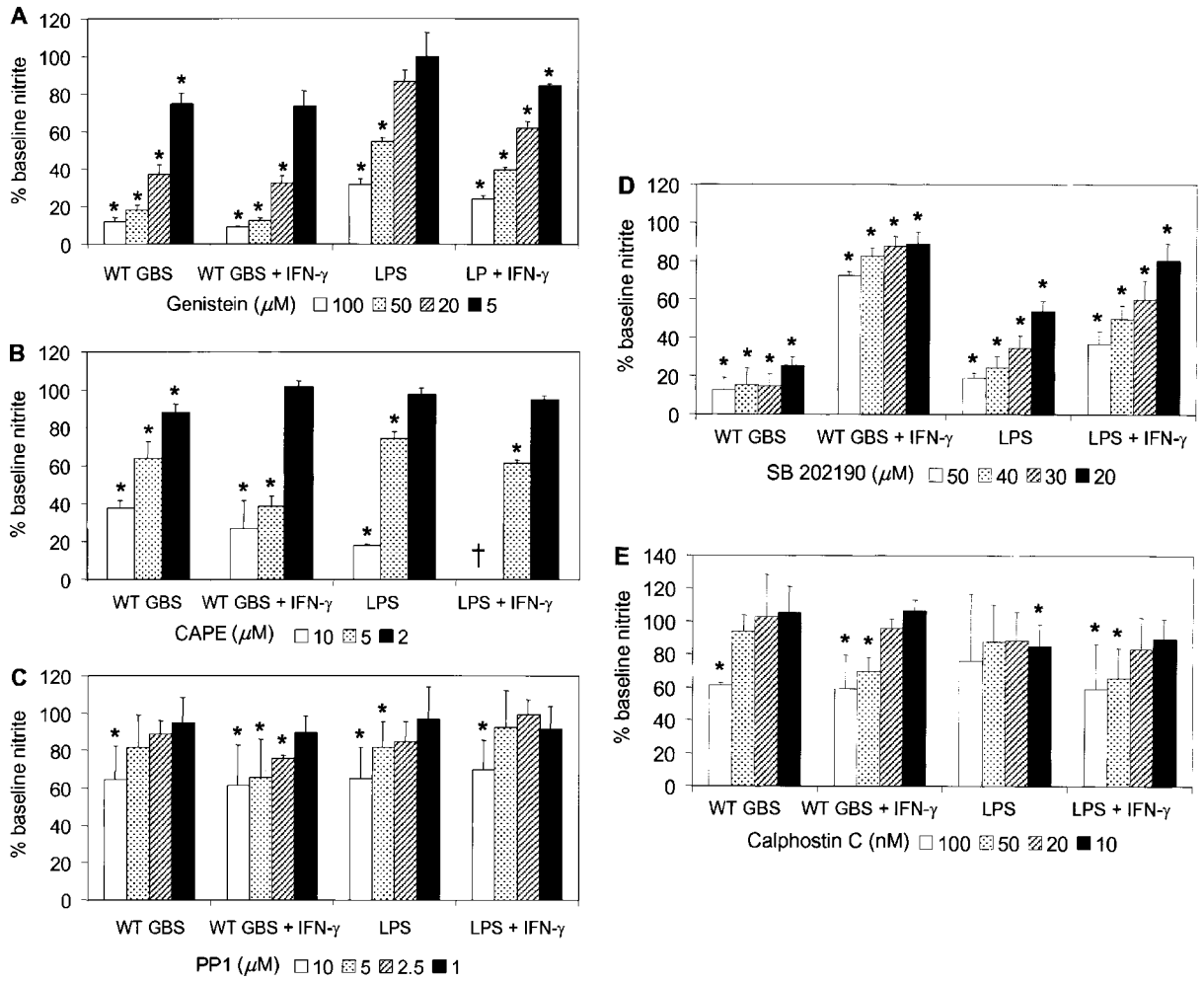

Figure 4. Dose-dependent inhibition of group B streptococcus (GBS)–activated nitrite formation in RAW 264.7 cells by selective inhibitors of signal transduction pathways. †, Indicates results were discarded because of cytotoxicity. Baseline nitrite values for cells without inhibitors (defined as 100% activity) were as follows: wild-type (WT) alone: 10.4 ± 5 μmol/L; WT and interferon (IFN)–γ: 25 ± 18 μmol/L; lipopolysaccharide (LPS) alone: 17.6 ± 5.5 μmol/L; LPS and IFN-γ: 30.8 ± 17 μmol/L. Data are mean ± SD of accumulated nitrite in culture medium in 3 independent experiments. Data for individual experiments are means of duplicate measurements. *Statistical significance ($P < .05$ by analysis of variance) vs. control measurements without inhibitor.

dithiocarbamate (PDTC; not shown) or caffeic acid phenethyl ester (CAPE; figure 4*B*), each an inhibitor of NF-κB activation. PDTC more effectively inhibited LPS-induced (66.5% ± 12.9%) compared with GBS-induced (30.3% ± 5.7%) NO production. Once again, at the concentrations used, neither substance resulted in loss of cell viability (data not shown).

Since inhibitors of tyrosine kinases and NF-κB attenuated the GBS-activated nitrite accumulation and NF-κB can be activated through a pathway involving *src* family tyrosine kinases, we tested the effect of PP1, a selective *src* kinase antagonist, on RAW 264.7 cell nitrite formation. PP1 mediated a dose-dependent partial inhibition of GBS- or LPS-induced nitrite accumulation and reached a maximum of 40% inhibition at concentrations up to 10 μ*M* (figure 4*C*). Higher concentrations were cytotoxic as detected by the MTT reduction or LDH release tests (data not shown).

Inflammatory activation of macrophages by LPS involves activation of the 3 mitogen-activated protein kinase (MAPK) families: extracellular signal-related kinase-1 and -2 (ERK-1/2, p42/44), p38 kinase, and c-Jun NH_2-terminal kinase (JNK). PD98059, a specific chemical inhibitor of ERK-1/2 phosphorylation by MAPK/ERK-1/2 (MEK-1 and MEK-2) [32], did not inhibit nitrite production of LPS- or GBS-challenged RAW 264.7 cells over a range of nontoxic concentrations (data not shown). In contrast, SB202190 (figure 4*D*) and SB203580 (not shown), selective inhibitors of p38 phosphorylation [33], both showed a concentration-dependent inhibition of nitrite formation in response to LPS or GBS. The inhibition was stronger

in the absence of IFN-γ, suggesting that treatment of the macrophages with 2 stimuli (IFN-γ plus LPS or GBS) might activate additional NO synthesis pathways not involving p38. Specific inhibitors of JNK kinases are currently not available.

To investigate whether the protein kinases A (PKA) or C (PKC) are involved in GBS-activated NO formation, we used the specific inhibitors H-89 (a PKA inhibitor) and calphostin C (a PKC inhibitor) in our assay. Even at doses of H-89 as high as 20 μM, nitrite formation or iNOS expression was not detectably reduced (data not shown). In contrast, calphostin C at high concentration mediated an ~40% reduction of GBS- or LPS-induced nitrite accumulation in the macrophage culture supernatants (figure 4*E*).

Effect of signal transduction inhibitors on iNOS expression by GBS-treated RAW 264.7 macrophages. The attenuation of GBS-induced nitrite accumulation afforded by the specific chemical inhibitors of protein tyrosine kinases, *src* kinases, p38 MAP kinase, NF-κB, and PKC was paralleled by decreased expression of iNOS protein as shown by Western blots (figure 5). However, only the NF-κB antagonist CAPE and the most potent tyrosine kinase antagonists, herbimycin A and tyrphostin AG126, blocked iNOS induction almost completely.

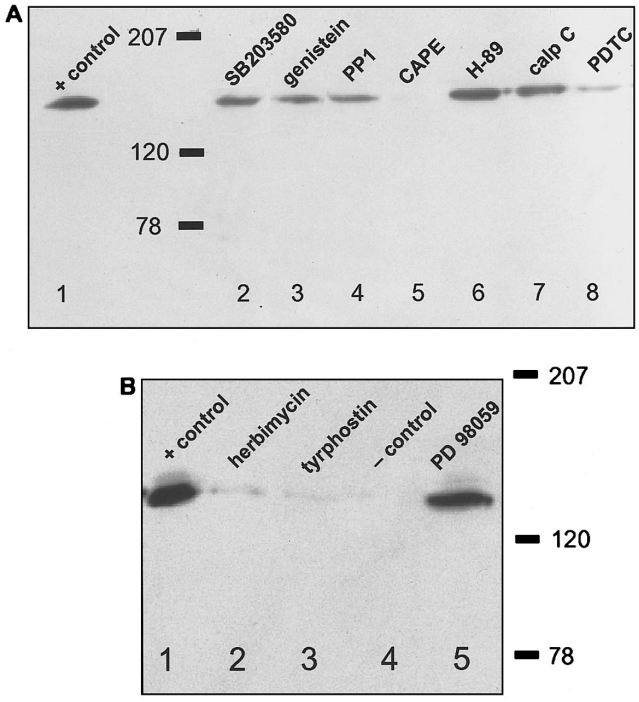

Figure 5. Blocking of group B streptococcus (GBS)–induced inducible nitric oxide synthase (iNOS) expression in RAW 264.7 macrophages by signal transduction inhibitors. *A,* Positive control (GBS without inhibitor), SB203580 (40 μM), genistein (50 μM), PP1 (20 μM), caffeic acid phenethyl ester (CAPE; 20 μM), H-89 (10 μM), calphostin C (100 nM), and pyrrolidine dithiocarbamate (PDTC; 20 μM). *B,* Positive control (GBS without inhibitor), herbimycin A (1 μM), tyrphostin AG 126 (50 μM), negative control (no treatment), and PD 98059 (40 μM).

Discussion

Although produced by the vast majority of GBS clinical isolates, the GBS β-hemolysin has yet to be fully characterized. One factor complicating analysis is that extracellular hemolytic activity is rapidly lost unless high-molecular-weight stabilizer molecules (albumin, starch, Tween 80) are present in the media [29]. Nonetheless, the development of isogenic NH and HH transposon mutants of GBS WT strains are powerful tools for exploration of the role of this exotoxin in various model systems of disease pathogenesis. Compared with the WT strain, HH mutants are more injurious and NH mutants less injurious to human lung epithelial cells [4], lung endothelial cells [5], brain endothelial cells [6], and, in the present study, murine macrophages. Genetic analysis of NH GBS mutants recently led to the identification of the GBS β-hemolysin locus, including the apparent structural gene for the hemolysin or hemolysin precursor [34, 35]. Cloning and expression of the GBS hemolysin [35], which shares no homology with other known bacterial toxins, promises to allow more-precise analysis of its mechanism(s) of action in the near future.

GBS hemolysin is associated with injury to lung epithelial and endothelial cells, which may explain the pulmonary hemorrhage and proteinaceous exudate characteristic of neonatal GBS pneumonia. Hemolysin inhibition by surfactant phospholipid may provide a rationale for the increased susceptibility of premature pulmonary surfactant-deficient neonates to GBS disease [4, 5]. However, mortality from early-onset GBS infection is most closely correlated with the hypotension, decreased tissue perfusion, and multiorgan failure seen in cases complicated by septic shock [36, 37]. Thus, we investigated whether the GBS β-hemolysin may also play a role in septic shock by examining its effect on an important early mediator of the sepsis syndrome—NO release by mononuclear cells.

Using isogenic NH and HH mutants of a virulent GBS clinical isolate, we found that the increase in nitrite elicited from RAW 264.7 cells by GBS correlated strongly with the expression of β-hemolysin. Treatment of macrophages with partially purified GBS hemolysin extracts also resulted in accumulation of nitrite and iNOS induction, but only if the hemolysin-stabilizing agents were present, confirming the role of the β-hemolysin. Macrophages treated with the NH mutant produced NO only at high doses (≥100 cfu/cell; data not shown). Likewise, supernatant extracts from the NH mutant containing stabilizing agents activated NO production at the 1:2 dilution, but not at higher dilutions. We did not investigate which components of GBS cause NO production in the absence of β-hemolysin; however, in other gram-positive bacterial species, high concentrations of LTA and peptidoglycan induce iNOS [38–40].

To further characterize the mechanism by which GBS β-hemolysin causes the expression of iNOS protein, we used signal

transduction inhibitors known to attenuate LPS- or LTA-induced iNOS expression. Proinflammatory mediators induce expression of iNOS via the transcription factor NF-κB [41]. We showed that PDTC and CAPE, inhibitors of NF-κB activation, strongly attenuated the expression of iNOS protein induced by GBS in RAW 264.7 cells. PDTC more effectively inhibited LPS-induced than GBS-induced nitrite accumulation, whereas CAPE was an equipotent antagonist of both LPS- and GBS-induced NO production.

Tyrosine kinase activation precedes NF-κB activation [42, 43], and tyrosine kinases play a role in LPS- and LTA-induced induction of iNOS [39, 44]. We demonstrated that three structurally distinct tyrosine kinase inhibitors, genistein (competitive inhibitor at the ATP binding site), tyrphostin AG126 (competitive inhibitor at the substrate binding site), and herbimycin A, inhibit the expression of iNOS caused by GBS. LPS-induced NO production was inhibited in a similar dose-dependent manner. In particular, *src* family tyrosine kinases, which are involved in LPS signaling mediated by CD14 [45], also appear to play a partial role in GBS-activated iNOS induction macrophages. Because the MAP kinases, ERK-1/2, p38, and JNK, are activated by LPS downstream of the *src* family kinases [46–51], we tested the effect of PD98059, a specific ERK-1/2 inhibitor, and SB202190/SB 203580, specific inhibitors of p38, on GBS-induced macrophage NO production. Of interest, only the stress-activated protein kinase p38, but not ERK-1/2, appears to be involved in GBS-mediated NO production. The inhibitory effects of the p38 antagonists, SB 202190 and SB203580, were less pronounced in IFN-γ–treated macrophages, suggesting that IFN-γ might activate additional signal transduction pathways that can bypass the p38 kinase. The concentration-dependent effects of SB202190 and SB203580 on GBS-activated NO release were comparable to LPS-induced NO production, suggesting that the intracellular pathways of LPS- and GBS-induced NO production converge early in the signal transduction cascade.

The intracellular signal transduction pathways leading to LPS- and GBS-activated NO release from macrophages appear to be highly conserved. The induction of iNOS by GBS does not appear to be due to contamination with LPS. Contaminating LPS was not detectable by the highly sensitive chromogenic LAL assay. In addition, polymyxin B, an agent that binds and inactivates LPS, abolished increases in nitrite caused by added LPS but not by GBS.

We recently reported that pneumolysin, a pore-forming, thiol-activated hemolysin of *S. pneumoniae,* induces iNOS in RAW 264.7 cells more potently than do pneumococcal cell wall preparations [25]. Prior to that report, iNOS-inducing activity had not been ascribed to a bacterial hemolysin. The results of the present study indicate that the GBS β-hemolysin, another pore-forming cytolysin, is also a potent inducer of iNOS expression and NO release in RAW 264.7 macrophages. Because recent data indicate the GBS β-hemolysin shares no genetic homology with pneumolysin or other bacterial hemolysin/cytolysins [35], receptor-specific signaling may not be required to initiate the process leading to hemolysin-induced NO production. We conclude that iNOS induction in mononuclear cells may be a common response to a variety of bacterial hemolysins and may contribute to the pathogenesis of bacterial septic shock.

Acknowledgment

We thank Michaela Leismann for excellent technical support with nitric oxide assays and Western blots.

References

1. Baker CJ, Edward MS. Group B streptococcal infections. In: Remington J, Klein JO, eds. Infectious diseases of the fetus and newborn infant, 4th ed. Philadelphia: WB Saunders, **1995**:980–1054.
2. Weiser JN, Rubens CE. Transposon mutagenesis of group B streptococcus beta-hemolysin biosynthesis. Infect Immun **1987**; 55:2314–6.
3. Rubens CE, Wessels MR, Heggen LM, Kasper DL. Transposon mutagenesis of type III group B streptococcus: correlation of capsule expression with virulence. Proc Natl Acad Sci USA **1987**; 84:7208–12.
4. Nizet V, Gibson RL, Chi EY, Framson PE, Hulse M, Rubens CE. Group B streptococcal beta-hemolysin expression is associated with injury of lung epithelial cells. Infect Immun **1996**; 64:3818–26.
5. Gibson RL, Nizet V, Rubens CE. Group B streptococcal β-hemolysin promotes injury of lung microvascular endothelial cells. Pediatr Res **1999**; 45:626–34.
6. Nizet V, Kim KS, Stins M, et al. Invasion of brain microvascular endothelial cells by group B streptococci. Infect Immun **1997**; 65:5074–81.
7. Griffiths BB, Rhee H. Effects of haemolysins of groups A and B streptococci on cardiovascular system. Microbios **1992**; 69:17–27.
8. Evans T, Carpenter A, Kinderman H, Cohen J. Evidence of increased nitric oxide production in patients with the sepsis syndrome. Circ Shock **1993**;41: 77–81.
9. Spack L, Havens PL, Griffith OW. Measurements of total plasma nitrite and nitrate in pediatric patients with the systemic inflammatory response syndrome. Crit Care Med **1997**; 25:1071–8.
10. Bucher M, Ittner KP, Zimmermann M, Wolf K, Hobhahn J, Kurtz A. Nitric oxide synthase isoform III gene expression in rat liver is up-regulated by lipopolysaccharide and lipoteichoic acid. FEBS Lett **1997**; 412:511–4.
11. Wong JM, Billiar TR. Regulation and function of inducible nitric oxide synthase during sepsis and acute inflammation. Adv Pharmacol **1995**; 34: 155–70.
12. Szabó C, Thiemermann C. Regulation of the expression of the inducible isoform of nitric oxide synthase. Adv Pharmacol **1995**; 34:113–53.
13. Geng Y, Maier R, Lotz M. Tyrosine kinases are involved with the expression of inducible nitric oxide synthase in human articular chondrocytes. J Cell Physiol **1995**; 163:545–54.
14. Okuda S, Kanda F, Kawahara Y, Chihara K. Regulation of inducible nitric oxide synthase expression in rat skeletal muscle cells. Am J Physiol **1997**; 272:C35–40.
15. Oddis CV, Simmons RL, Hattler BG, Finkel MS. Protein kinase A activation is required for IL-1–induced nitric oxide production by cardiac myocytes. Am J Physiol **1996**; 271:C429–34.
16. Kleinert H, Euchenhofer C, Ihrig-Biedert I, Förstermann U. In murine 3T3 fibroblasts, different second messenger pathways resulting in the induction of NO synthase II (iNOS) converge in the activation of transcription factor NF-κB. J Biol Chem **1996**; 271:6039–44.
17. Singh K, Balligand J, Fischer TA, Smith TW, Kelly RA. Regulation of cy-

tokine-inducible nitric oxide synthase in cardiac myocytes and microvascular endothelial cells. J Biol Chem **1996**;271:1111–7.

18. Kitamura Y, Takahashi H, Nomura Y, Taniguchi T. Possible involvement of Janus kinase Jak2 in interferon-γ induction of nitric oxide synthase in rat glial cells. Eur J Pharmacol **1996**;306:297–306.
19. Milbourne EA, Bygrave FL. Does nitric oxide play a role in liver function? Cell Signal **1995**;7:313–8.
20. Kitamura K, Singer WD, Star RA, Muallem S, Miller RT. Induction of inducible nitric oxide synthase by the heterotrimeric G protein $G\alpha_{13}$. J Biol Chem **1996**;271:7412–5.
21. Kilbourn RG, Szabó C, Traber DL. Beneficial versus detrimental effects of nitric oxide synthase inhibitors in circulatory shock: lessons learned from experimental and clinical studies. Shock **1997**;7:235–46.
22. Suttorp N, Fuhrmann M, Tannert-Otto S, Grimminger F, Bhakdi S. Pore-forming bacterial toxins potently induce release of nitric oxide in porcine endothelial cells. J Exp Med **1993**;178:337–41.
23. Schütte H, Mayer K, Gessler T, et al. Nitric oxide biosynthesis in an exotoxin-induced septic lung model. Am J Respir Crit Care Med **1998**;157:498–504.
24. Goodrum KJ, McCormick LL, Schneider B. Group B streptococcus-induced nitric oxide production is CR3 (CD 11b/CD18) dependent. Infect Immun **1994**;62:3102–7.
25. Braun JS, Novak R, Gao G, Murray PJ, Shenep J. Pneumolysin, a protein toxin from *Streptococcus pneumoniae,* induces nitric oxide production from macrophages. Infect Immun **1999**;67:3750–6.
26. Alouf JE, Geoffroy C. The family of the antigenically-related, cholesterol-binding ('sulphydryl-activated') cytolytic toxins. In: Alouf JE, Freer JH, eds. Sourcebook of bacterial protein toxins. London: Academic Press, **1991**:147–86.
27. Lacks S, Hotchkiss RD. A study of the genetic material determining an enzyme activity in pneumococcus. Biochem Biophys Acta **1960**;39:508–17.
28. Wessels MR, Benedi V, Kasper DL, Heggen LM, Rubens CE. Type III capsule and virulence of group B streptococci. In: Dunny GM, Cleary PP, McKay LL eds. Genetics and molecular biology of streptococci, lactococci, and enterococci. Washington, DC: American Society for Microbiology, **1991**: 219–23.
29. Marchlewicz BA, Duncan JL. Properties of a hemolysin produced by group B streptococci. Infect Immun **1980**;30:805–13.
30. Hevel J, Marletta M. Nitric-oxide synthase assays. Methods Enzymol **1994**;233:250–8.
31. Mosmann T. Rapid colorimetric assay for cellular growth and survival: application to proliferation and cytotoxicity assays. J Immunol Methods **1983**;65:55–63.
32. Pang L, Sawada T, Decker SJ, Saltiel AR. Inhibition of MAP kinase blocks the differentiation of PC-12 cells induced by nerve growth factor. J Biol Chem **1995**;270:13585–8.
33. Hwang D, Jang BC, Yu G, Boudreau M. Expression of mitogen-inducible cyclooxygenase induced by lipopolysaccharide. Biochem Pharmacol **1997**;54:87–96.
34. Spellerberg B, Pohl B, Haase G, Martin S, Weber-Heynemann J, Lütticken R. Identification of genetic determinants for the hemolytic activity of *Streptococcus agalactiae* by IS*S1* transposition. J Bacteriol **1999**;181: 3212–9.
35. Pritzlaff CA, Chang JCW, Tamura GS, Rubens CE, Nizet V. Genetic basis of the group B streptococcal β-hemolysin/cytolysin. In: Martin DR, Tagg JR, eds. Streptococci and streptococcal diseases—entering the new millennium: proceedings of the 14th Lancefield International Symposium on Streptococci and Streptococcal Diseases (Auckland, NZ). Auckland, NZ: Securacopy (in press).
36. Lannering B, Larsson LE, Rogas J, et al. Early onset group B streptococcal disease. Seven year experience and clinical scoring system. Acta Paediatr Scand **1983**;72:597–602.
37. Payne NR, Burke BA, Day DL, Christenson PD, Thompson TR, Ferrieri P. Correlation of clinical and pathologic findings in early onset neonatal group B streptococcal infection with disease severity and prediction of outcome. Pediatr Infect Dis J **1988**;7:836–47.
38. Kengatharan M, De Kimpe SJ, Thiemermann C. Analysis of the signal transduction in the induction of nitric oxide synthase by lipoteichoic acid in macrophages. Br J Pharmacol **1996**;117:1163–70.
39. Hattor Y, Kasai K, Akimoto K, Thiemermann C. Induction of NO synthesis by lipoteichoic acid from *Staphylococcus aureus* in J774 macrophages: involvement of a CD14-dependent pathway. Biochem Biophys Res Commun **1997**;233:375–9.
40. De Kimpe SJ, Kengatharan M, Thiemermann C. The cell wall components peptidoglycan and lipoteichoic acid from *Staphylococcus aureus* act in synergy to cause shock and multiple organ failure. Proc Natl Acad Sci USA **1995**;92:10359–63.
41. Xie QW, Kashiwabara Y, Nathan C. Role of transcription factor NF-κB/Rel in induction of nitric oxide synthase. J Biol Chem **1994**;269:4705–8.
42. Read MA, Cordle SR, Veach RA, Carlisle CD, Hawiger J. Cell-free pool of CD-14 mediates activation of transcription factor NF-κB by lipopolysaccharide in human endothelial cells. Proc Natl Acad Sci USA **1993**;90: 9887–91.
43. Iwasata T, Uehara Y, Graves L, Rachie N, Bonsztyk K. Herbimycin A blocks IL-1 induced NF-κB DNA-binding activity in lymphoid cell lines. FEBS Lett **1992**;298:240–4.
44. Paul A, Plevin R. Cell signalling events involved in mediating the induction of nitric oxide synthase in macrophages and vascular smooth muscle cells. Biochem Soc Trans **1995**;23:1029–33.
45. Stefanova I, Corcoran ML, Horak EM, Wahl LM, Bolen JB, Horak ID. Lipopolysaccharide induces activation of CD14-associated protein tyrosine kinase p53/56lyn. J Biol Chem **1993**;268:20725–8.
46. Liu KM, Herrera P, Brownsey RW, Reiner NE. CD14-dependent activation of protein kinase C and mitogen-activated protein kinases (p42 and p44) in human monocytes treated with bacterial lipopolysaccharide. J Immunol **1994**;153:2642–52.
47. Hambleton J, Weinstein SL, Lem L, De Franco AL. Activation of c-Jun N-terminal kinase in bacterial lipopolysaccharide-stimulated macrophages. Proc Natl Acad Sci USA **1996**;93:2774–8.
48. Han J, Lee JD, Tobias PS, Ulevitch RJ. Endotoxin induces rapid protein tyrosine phosphorylation in 70Z/3 cells expressing CD14. J Biol Chem **1993**;268:25009–14.
49. Han J, Lee JD, Bibbs L, Ulevitch RJ. A MAP kinase targeted by endotoxin and hyperosmolarity in mammalian cells. Science **1994**;265:808–11.
50. Sanghera JS, Weinstein SL, Aluwalia M, Girn J, Pelech SL. Activation of multiple proline-directed kinases by bacterial lipopolysaccharide in murine macrophages. J Immunol **1996**;156:4457–65.
51. Li JD, Feng W, Gallup M, et al. Activation of NF-κB via a Src-dependent Ras-MAPK-pp90rsk pathway is required for *Pseudomonas aeruginosa*–induced mucin overproduction in epithelial cells. Proc Natl Acad Sci USA **1998**;95:5718–23.